ROBOTIC CONTROL OF THE SEVEN-DEGREE-OF-FREEDOM NASA LABORATORY TELEROBOTIC MANIPULATOR*

R. V. Dubey, J. A. Euler and R. B. Magness
Mechanical & Aerospace Engineering
The University of Tennessee
Knoxville, Tennessee 37996

S. M. Babcock and J. N. Herndon
Oak Ridge National Laboratory
Oak Ridge, Tennessee 37831

ABSTRACT

A computationally efficient robotic control scheme for the NASA Laboratory Telerobotic Manipulator (LTM) is presented. This scheme utilizes the redundancy of the seven-degree-of-freedom LTM to avoid joint limits and singularities. An analysis to determine singular configurations is presented. Performance criteria are determined based on the joint limits and singularity analysis. The control scheme is developed in the framework of resolved rate control using the gradient projection method, and it does not require the generalized inverse of the Jacobian. An efficient formulation for determining the joint velocities of the LTM is obtained. This control scheme is well suited for real-time implementation, which is essential if the end-effector trajectory is continuously modified based on sensory feedback. Implementation of this scheme on a Motorola 68020 VME bus-based controller of the LTM is in progress. Simulation results demonstrating the redundancy utilization in the robotic mode are presented.

1. Introduction

NASA has embarked on an extensive national project to establish a permanent human-occupied space station. To accomplish this project, significantly increased levels of dexterous human-like handling tasks will be required in orbit. This will include space station construction as well as planned and unplanned maintenance operations on the station. In addition, a significant amount of satellite repair and maintenance is expected in the future. To meet the need for sharply increased levels of dexterous handling while decreasing the levels of required human extravehicular activity, NASA has established a goal for significant use of telerobotic hardware in future space activities.

The NASA Langley Research Center has sponsored the Laboratory Telerobotic Manipulator (LTM) Prototype Project at the Oak Ridge National Laboratory to develop prototypical manipulators for use in NASA laboratories to develop and demonstrate telerobotic and robotic capabilities in an earth-based environment [1]. As a result, the LTM must be designed to be a high-quality force-reflecting teleoperator with capabilities for robotic operation. High performance under human control, low required backdriving torque, high velocity and acceleration capability, and good capacity-to-weight ratio are emphasized in the design. To provide the basis for a transition to autonomous robotic operation, features for high-quality robotic operation are also provided. These include good end-effector positioning accuracy and high mechanical and control stiffness. The LTM is also designed for modular maintainability to ease repair and reconfiguration.

The LTM arm, shown in Fig. 1, has seven degrees of freedom that provide kinematic redundancy. The arm is configured from three common pitch/yaw joints which combine to provide shoulder, elbow, and wrist joints. The

*Research performed at Oak Ridge National Laboratory, operated by Martin Marietta Energy Systems, Inc., for the U.S. Department of Energy under Contract No. DE-AC05-840R21400, and sponsored by the National Aeronautics and Space Administration, Langley Research Center.

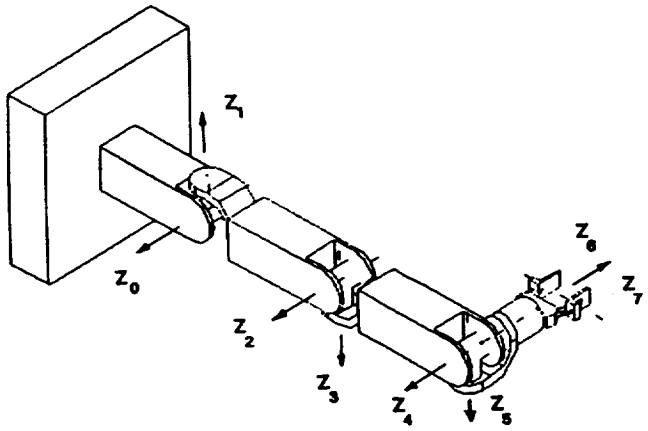

Fig.1 Laboratory Telerobotic Manipulator

Table 1. Denavit-Hartenberg table of link parameters

θ_i (deg)	d_i (m)	α_i (deg)	a_i (m)	θ_i (deg) shown
θ_1	0	-90	0	-90
θ_2	0	90	a_2	0
θ_3	0	90	0	90
θ_4	0	-90	a_4	0
θ_5	0	90	0	0
θ_6	0	90	0	90
θ_7	d_7	0	0	0

Note: a_2 = 23.0 in., a_4= 20.0 in., d_7 = 12.0 in.

Table 2. Motion Range of the LTM
(Note: Zero reference is indicated in Figure 1)

Motion	Range (degrees) with counterbalancing and with cabling	Range (degrees) without counterbalancing and with cabling
Shoulder pitch	$-45 > \theta_1 > -135$	$+30 > \theta_1 > -135$
Shoulder yaw	$+180 > \theta_2 > -180$	$+180 > \theta_2 > -180$
Elbow pitch	$+120 > \theta_3 > +45$	$+135 > \theta_3 > -30$
Elbow yaw	$+120 > \theta_4 > -120$	$+180 > \theta_4 > -180$
Wrist pitch	$+135 > \theta_5 > -30$	$+135 > \theta_5 > -30$
Wrist yaw	$+180 > \theta_6 > 0$	$+180 > \theta_6 > 0$
Wrist roll	$+180 > \theta_7 > -180$	$+180 > \theta_7 > -180$

interface boundaries of these joints provide inherent modularity. A wrist roll mechanism, mounted on the output of the wrist joint, provides the seventh degree of freedom. Seven degrees of freedom allow the LTM to reorient itself without changing the end-effector position and orientation. This paper describes the robotic control scheme for the LTM for utilizing redundancy to avoid internal singularities and joint limits.

2. Robotic Control of the LTM

Several joints of a robotic manipulator at time-varying rates simultaneously move the end-effector along a specified path defined in terms of end-effector position and orientation as a function of time. In the case of a six-degree-of-freedom manipulator, joint motions required to achieve a specified end-effector motion are unique. However, a seven-or more degree-of-freedom manipulator has more joints than the six independent variables required to completely specify the position and orientation of the end-effector. The kinematic linear equations relating unknown joint velocities to specified end-effector velocity components do not have unique solutions–an infinite number of solutions is possible. Thus we may choose a joint velocity solution that results in "improved" performance of the manipulator while tracking a desired trajectory, and performance may be judged by criteria such as avoiding obstacles or joint limits.

A number of control schemes for determining joint trajectories for redundant manipulators have been suggested by researchers. Most control schemes in the literature determine joint velocities through global or local optimization of various performance criteria. Global optimization schemes are generally iterative and computationally complex; thus, they are currently limited to off-line programming. On-line implementation is essential if the end-effector trajectory is continuously modified based on sensory feedback. Most local optimization schemes are presented in the framework of resolved rate control [2]. Control of the LTM in the robotic mode is achieved by an efficient gradient projection kinematic control scheme developed by Dubey et al. [3]. This scheme avoids computation of the pseudoinverse of the Jacobian, and it results in an efficient formulation for determining joint velocities.

3. Kinematic Optimization Scheme

The kinematic optimization scheme developed by Dubey et al. [3] used to control the LTM can be summarized as follows. A manipulator using n joints to control m independent variables of the end-effector position and orientation ($m \leq 6$) is described by the following kinematic equation:

$$\dot{x} = J\dot{\theta} \ , \tag{1}$$

where $\dot{x}$ is an m-dimensional vector of linear and angular velocities of the end-effector with reference to base coordinates, $\dot{\theta}$ is an n-dimensional vector of joint velocities, and J is an $m \times n$ Jacobian matrix.

If J is a square matrix and has full rank, then the joint velocities required to achieve the desired end-effector motion will be unique and can be evaluated by

$$\dot{\theta} = J^{-1}\dot{x} \ . \tag{2}$$

If J is rectangular with $m < n$, the joint velocities can be computed by

$$\dot{\theta} = J^{+}\dot{x} + (I - J^{+}J)\dot{\phi} \ , \tag{3}$$

where J^{+} is the Moore-Penrose generalized inverse [4] of the Jacobian. If J has a full rank , then

$$J^{+} = J^{T}(JJ^{T})^{-1}. \tag{4}$$

The matrix I in Eq. (3) is an $n \times n$ identity matrix, and the vector $\dot{\phi}$ is an arbitrary n-dimensional joint velocity vector. To optimize a performance criterion $H(\theta)$ using the gradient projection method [5], redundancy is resolved by substituting $k\nabla H(\theta)$ for $\dot{\phi}$ in Eq. (3) and rewriting it as

$$\dot{\theta} = J^{+}\dot{x} + k(I - J^{+}J)\nabla H(\theta). \tag{5}$$

The coefficient k in Eq. (5) is a real scalar constant, and $\nabla H(\theta)$ is the gradient vector of $H(\theta)$.

Let $\dot{\theta} \in R^{7}$ be the joint velocity vector for the seven-degree-of-freedom manipulator. Suppose in the Cartesian workspace the end-effector velocity is described by a six-dimensional vector with reference to the base coordinates, and has three linear and three angular velocity components. The joint velocity vector $\dot{\theta}$ and the end-effector velocity vector $\dot{x}$ are related by Eq. (1), where J is a 6×7 Jacobian matrix. We will assume that the rank of the Jacobian is six, which implies that J is not singular. Thus, it is possible to construct a nonsingular 6×6 matrix J^{*} from any six independent columns of the matrix. In general, by rearranging the columns of J and the corresponding elements of $\dot{\theta}$ in a different order, we can rewrite Eq. (1) as

$$\dot{x} = [\alpha \ J^{*}]\dot{\theta} \ , \tag{6}$$

where α is any column vector of the Jacobian such that the remaining six columns form a nonsingular matrix J^{*}. Rearranging terms in Eq. (5), we obtain the following:

$$\dot{\theta} = J^{+}(\dot{x} - kJ\nabla H) + k\nabla H \ . \tag{7}$$

A suitable selection of k may be based on the hardware bounds on the joint velocities and heuristics. The first term on the right-hand side of Eq. (7) is the least-norm solution of Eq. (1) with $\dot{x}$ replaced by $(\dot{x} - kJ\nabla H)$. As shown in ref.3, the least-norm solution can be obtained from a particular solution $\dot{\theta}^{*}_{p}$ and a homogeneous solution $\dot{\theta}^{*}_{h}$ of this equation by subtracting from the particular solution its component along the homogeneous solution. Thus we have

$$\dot{\theta} = \dot{\theta}^{*}_{p} - \left(\frac{\dot{\theta}^{*T}_{p} \ \dot{\theta}^{*}_{h}}{\dot{\theta}^{*T}_{h} \ \dot{\theta}^{*}_{h}} \right) \dot{\theta}^{*}_{h} + k\nabla H \ , \tag{8}$$

where

$$\dot{\theta}_p^* = \begin{bmatrix} 0 \\ J^{*-1}(\dot{x} - kJ\nabla H) \end{bmatrix}, \tag{9}$$

and

$$\dot{\theta}_h^* = \begin{bmatrix} 1 \\ J^{*-1}\alpha \end{bmatrix}. \tag{10}$$

If we assume the wrist to be spherical, with none of the two wrist axes pairs aligned, we can partition J^* as follows:

$$J^* = \begin{bmatrix} J_1^{*3x3} & 0^{3x3} \\ J_2^{*3x3} & J_3^{*3x3} \end{bmatrix}. \tag{11}$$

To determine $J^{*-1}(\dot{x} - kJ\nabla H)$ and $J^{*-1}\alpha$ in Eqs. (9) and (10) respectively, we need only to solve two sets of three simultaneous equations. Thus a simple formulation for determining the joint velocities is obtained.

4. Inverse Kinematics of the LTM

The above control scheme for optimizing a performance criterion using the gradient projection method was applied to the LTM. The LTM is a seven degree-of-freedom manipulator with a spherical wrist. The pitch-yaw-roll spherical wrist is designed so that its singularities occur when the hand is pointing to its sides and at the extremes of motion range, not when it is pointing straight out, as is common in many industrial manipulators. Degrees of freedom of the LTM and the coordinate frames referred to in the Denavit-Hartenberg table (Table 1) for this manipulator are shown in Fig.1.

To simplify the calculations, we will refer the desired end-effector and wrist velocity vectors to the third coordinate frame x_3, y_3, z_3, which is attached to link 3 using the notation used by Paul [6]. This results in a Jacobian that has a much simpler form and thus is more efficient for computation. Let the desired end-effector velocity referred to the third coordinate frame be given by

$$\begin{aligned} {}^3\dot{x}_h &= [\,{}^3v_h^T \quad {}^3\omega_h^T\,]^T \\ {}^3\dot{x}_h &= [{}^3v_{h_1}\ {}^3v_{h_2}\ {}^3v_{h_3}\ {}^3\omega_{h_1}\ {}^3\omega_{h_2}\ {}^3\omega_{h_3}]^T, \end{aligned} \tag{12}$$

where ${}^3v_h \in R^3$ and ${}^3\omega_h \in R^3$ are the linear and angular hand velocity vectors, respectively, referred to the third coordinate frame.

Let the desired wrist velocity vector referred to the third coordinate frame be given by

$$\begin{aligned} {}^3\dot{x}_w &= [\,{}^3v_w^T \quad {}^3\omega_w^T\,]^T \\ {}^3\dot{x}_w &= [{}^3v_{w_1}\ {}^3v_{w_2}\ {}^3v_{w_3}\ {}^3\omega_{w_1}\ {}^3\omega_{w_2}\ {}^3\omega_{w_3}]^T, \end{aligned} \tag{13}$$

where ${}^3v_w \in R^3$ and ${}^3\omega_w \in R^3$ are the linear and angular wrist velocity vectors, respectively, referred to the third coordinate frame. For a given ${}^3\dot{x}_h$, the terms of ${}^3\dot{x}_w$ may be obtained by using the following relationships:

$${}^3\omega_w = {}^3\omega_h, \tag{14}$$

$$ {}^3v_w = {}^3v_h - {}^3\omega_h \times d_7\, {}^3z_h , \tag{15} $$

where ${}^3z_h$ is the unit vector z_h at the hand (Fig. 1) that is referred to the third coordinate frame; ${}^3z_h$ may be shown to be the following:

$$ {}^3z_h = \left[s_4c_6+c_4c_5s_6 \;\; s_4c_5s_6-c_4c_6 \;\; -s_5s_6 \right]^T , \tag{16} $$

where c_i and s_i represent $\cos\theta_i$ and $\sin\theta_i$ respectively. Let ${}^3J_w$ be the Jacobian relating the joint velocity vector $\dot{\theta} = [\dot{\theta}_1, \dot{\theta}_2, \ldots, \dot{\theta}_7]^T$ and the wrist velocity vector ${}^3\dot{x}_w$ such that

$$ {}^3\dot{x}_w = {}^3J_w\dot{\theta} . \tag{17} $$

The Jacobian ${}^3J_w$ can be shown to be the following:

$$ {}^3J_w = \begin{bmatrix} a_4s_2s_3s_4+a_2c_2s_3 & a_4c_3s_4 & 0 & -a_4s_4 & 0 & 0 & 0 \\ -a_4s_2s_3c_4 & -a_4c_3c_4-a_2 & 0 & a_4c_4 & 0 & 0 & 0 \\ -a_4(s_2c_3s_4+c_2c_4)-a_2c_2c_3 & a_4s_3s_4 & -a_4c_4 & 0 & 0 & 0 & 0 \\ -s_2c_3 & s_3 & 0 & 0 & -s_4 & c_4s_5 & c_4c_5s_6+s_4c_6 \\ c_2 & 0 & 1 & 0 & c_4 & s_4s_5 & s_4c_5s_6-c_4c_6 \\ -s_2s_3 & -c_3 & 0 & 1 & 0 & c_5 & -s_5s_6 \end{bmatrix} , \tag{18} $$

where, as before, c_i and s_i represent $\cos\theta_i$ and $\sin\theta_i$ respectively.

To determine the joint velocities required to follow a desired end-effector velocity and to optimize a given performance criterion using the gradient projection method, we first determine the end-effector velocity ${}^3\dot{x}_h$ referred to the third coordinate frame. Given the end-effector velocity vector $\dot{x}_h \in R^6$ in the base coordinates, we can determine ${}^3\dot{x}_h$ from the following:

$$ {}^3\dot{x}_h = {}^3R_0\dot{x}_h , \tag{19} $$

where ${}^3R_0$ is a 3×3 projection matrix given by

$$ {}^3R_0 = \begin{bmatrix} c_1c_2c_3-s_1s_3 & s_1c_2c_3+c_1s_3 & -s_2c_3 \\ c_1s_2 & s_1s_2 & c_2 \\ c_1c_2s_3+s_1c_3 & s_1c_2s_3-c_1c_3 & -s_2s_3 \end{bmatrix} , \tag{20} $$

and c_i and s_i represent $\cos\theta_i$ and $\sin\theta_i$ respectively. We can now determine wrist velocity vector ${}^3\dot{x}_w$ from Eqs. (14) and (15).

Consider the case when the first column of the Jacobian is taken to be α and the remaining six columns are independent and form the matrix J^*. The elements of $\dot{\theta}^*_p$ denoted by $\dot{\theta}^*_{p_i}$, for i = 1 to 7, with $\dot{\theta}^*_{p_1} = 0$, may be obtained as follows:

$$ \begin{bmatrix} \dot{\theta}^*_{p2} \\ \dot{\theta}^*_{p4} \end{bmatrix} = \frac{1}{\Delta} \begin{bmatrix} a_4c_4 & a_4s_4 \\ a_2+a_4c_3c_4 & a_4c_3s_4 \end{bmatrix} \begin{bmatrix} \dot{x}_1 \\ \dot{x}_2 \end{bmatrix} , \tag{21a} $$

where $\Delta = -a_2a_4s_4$,

$$\dot{\theta}^*_{p3} = \frac{(a_4s_3s_4)\dot{\theta}^*_{p2} - \dot{x}_3}{a_4c_4} , \tag{22a}$$

$$\begin{bmatrix} \dot{\theta}^*_{p5} \\ \dot{\theta}^*_{p6} \\ \dot{\theta}^*_{p7} \end{bmatrix} = \frac{1}{s_6} \begin{bmatrix} c_4c_5c_6-s_4s_6 & s_4c_5c_6+c_4s_6 & -s_5c_6 \\ c_4s_5s_6 & s_4s_5s_6 & c_5s_6 \\ c_4c_5 & s_4c_5 & -s_5 \end{bmatrix} \begin{bmatrix} \dot{x}_4 - s_3\dot{\theta}^*_{p2} \\ \dot{x}_5 - \dot{\theta}^*_{p3} \\ \dot{x}_6 + c_3\dot{\theta}^*_{p2} - \dot{\theta}^*_{p4} \end{bmatrix} . \tag{23a}$$

On the other hand, another column, say column four, may be taken to be α with the remaining six columns forming the matrix $\mathbf{J}^*$, in which case if $\mathbf{J}^*$ is nonsingular we have $\dot{\theta}^*_{p4} = 0$ and :

$$\begin{bmatrix} \dot{\theta}^*_{p1} \\ \dot{\theta}^*_{p2} \end{bmatrix} = \frac{1}{\Delta} \begin{bmatrix} -(a_2+a_4c_3c_4) & -a_4c_3s_4 \\ a_4s_2s_3c_4 & a_4s_2s_3s_4+a_2c_2s_3 \end{bmatrix} \begin{bmatrix} \dot{x}_1 \\ \dot{x}_2 \end{bmatrix} , \tag{21b}$$

where $\Delta = -a_2s_3(a_4c_2c_3c_4 + a_4s_2s_4 + a_2c_2)$,

$$\dot{\theta}^*_{p3} = \frac{(a_4s_3s_4)\dot{\theta}^*_{p2} - \dot{x}_3 - [a_4(s_2c_3s_4 + c_2c_4) + a_2c_2c_3]\dot{\theta}^*_{p1}}{a_4c_4} , \tag{22b}$$

and

$$\begin{bmatrix} \dot{\theta}^*_{p5} \\ \dot{\theta}^*_{p6} \\ \dot{\theta}^*_{p7} \end{bmatrix} = \frac{1}{s_6} \begin{bmatrix} c_4c_5c_6-s_4s_6 & s_4c_5c_6+c_4s_6 & -s_5c_6 \\ c_4s_5s_6 & s_4s_5s_6 & c_5s_6 \\ c_4c_5 & s_4c_5 & -s_5 \end{bmatrix} \begin{bmatrix} \dot{x}_4 + s_2c_3\dot{\theta}^*_{p1} - s_3\dot{\theta}^*_{p2} \\ \dot{x}_5 - c_2\dot{\theta}^*_{p1} - \dot{\theta}^*_{p3} \\ \dot{x}_6 + s_2s_3\dot{\theta}^*_{p1} + c_3\dot{\theta}^*_{p2} \end{bmatrix} . \tag{23b}$$

In Eqs. (21) through (23), $\dot{x}_i$ for i = 1 to 6 are the i^{th} elements of the vector $(\dot{x} - k\mathbf{J}\nabla H)$. The vector $\dot{\theta}^*_h$ with elements $\dot{\theta}^*_{h\,i}$, i = 1 to 7, may similarly be obtained by setting the element $\dot{\theta}^*_{h\,i} = 1$, where i = 1 for the case when α is taken to be the first column and i = 4 when α is taken to be the fourth column. The remaining elements of $\dot{\theta}^*_h$ may be obtained from Eqs. (21) through (23) by replacing $\dot{\theta}^*_{p\,i}$ by $\dot{\theta}^*_{h\,i}$ and using the i^{th} elements of vector $-\alpha$ for $\dot{x}_i$ for i = 1 to 6.

We have obtained computationally efficient closed-form solutions for the elements of $\dot{\theta}^*_p$ and $\dot{\theta}^*_h$ in Eqs. (21) through (23). The vector $\dot{\theta}$ can now be obtained from Eq. (8). Thus, by this approach we have eliminated the need to determine the generalized inverse of the Jacobian or to numerically solve the six simultaneous equations with six unknowns. Suppose that in the course of execution we have s_4 approaching zero, then α may be chosen to be equal to column 4. On the other hand, if s_3 approaches zero we may choose α to be column 1. In all cases, $c_4 = 0$ and/or $s_6 = 0$ must be avoided, situations achieved by optimizing a suitable performance criterion.

5. Performance Criteria and Singularity Analysis

To avoid joint limits and singular configurations of the LTM we have developed performance criteria to be optimized using the control scheme presented in the last section. The motion ranges of the joints of the LTM, given in Table 2, are given for two cases: (1) with counter-balancing and cabling and (2) without counter-balancing and with cabling (see Fig.1). To stay within the joint limits specified in Table 2, we may choose the following performance criterion:

$$H(\theta) = \Sigma\,(\theta_i - \theta_{imid})^2 \ , \tag{24}$$

where θ_i is the i^{th} joint angle and θ_{imid} is the midpoint value for the θ_i joint angle. Inspection of the above performance criterion shows that if it is minimized, the joint angles tend to stay in their midrange. Each term in the above summation may be weighted according to the range of the corresponding joint motion and its distance from the midpoint.

When a manipulator is in a singular configuration it is unable to move or rotate the end-effector in at least one direction. The joint velocities required to move in this direction are infinitely high. In a configuration close to a singular configuration joint velocities required to move in certain direction(s) are much above the hardware bounds on joint velocities, resulting in inaccurate motion. The workspace of an articulated manipulator (redundant or nonredundant) is filled with singularities at the workspace boundaries as well as inside the workspace. Singularities at the workspace boundaries are usually unavoidable; however, singularities inside the workspace, referred to as internal singularities, are avoidable for manipulators with redundant joints. Because an infinite number of joint configurations results in a given position and orientation of a redundant manipulator within its workspace, it is possible to choose a nonsingular joint configuration. However, in order to avoid singular configurations we need to know the conditions for singularity.

When a manipulator is in a singular configuration, the determinant of $\mathbf{J}\mathbf{J}^T$ is zero [7]. Thus the joint coordinates that make the determinant of $\mathbf{J}\mathbf{J}^T$ equal to zero would result in singular configurations. However, this condition involves an extremely complicated equation which is difficult to solve. The singularities of a seven-degree-of-freedom arm such as the LTM occur when the rank of the Jacobian $\mathbf{J}$ is less than six, implying that the arm is in a configuration in which the end-effector cannot be moved and rotated in a completely arbitrary direction. Because the Jacobian for the LTM is a 6×7 matrix, the rank of it may be determined by considering the determinant of all seven 6×6 matrices that can be formed from the columns of $\mathbf{J}$. Since this determination is extremely laborious, we utilize the following scheme.

When joint 6 is either 0 or 180°, then joint 5 is collinear with joint 7. In this case the column 5 vector of $\mathbf{J}$ is equal to or the negative of the column 7 vector, which implies that the wrist is singular and cannot be moved to an arbitrary new orientation with just the use of the wrist joint angles. Thus, the task of finding the singularities has been broken into two parts. The singularities will be considered first for the case when joints 5 and 7 are not collinear, and then for the case when joints 5 and 7 are collinear. The Jacobian referred to the second coordinate frame ${}^2\mathbf{J}$ contains the following components:

$$ {}^2\mathbf{J} = \begin{bmatrix} -a_4c_2s_3c_4 & a_4s_4 & -a_4s_3c_4 & -a_4c_3s_4 & 0 & 0 & 0 \\ a_4(s_2s_4+c_2c_3c_4)+a_2c_2 & 0 & a_4c_3c_4 & -a_4s_3s_4 & 0 & 0 & 0 \\ -a_4s_2s_3c_4 & -(a_2+a_4c_3c_4) & 0 & a_4c_4 & 0 & 0 & 0 \\ -s_2 & 0 & 0 & s_3 & -c_3s_4 & c_3c_4s_5+s_3c_5 & (c_3c_4c_5-s_3s_5)s_6+c_3s_4c_6 \\ 0 & 1 & 0 & -c_3 & -s_3s_4 & s_3c_4s_5-c_3c_5 & (s_3c_4c_5+c_3s_5)s_6+s_3s_4c_6 \\ c_2 & 0 & 1 & 0 & c_4 & s_4s_5 & s_4c_5s_6-c_4c_6 \end{bmatrix} \tag{25} $$

We now consider the following the cases:

1. Joints 5 and 7 Are Not Collinear (Nonsingular Wrist)

Since the wrist is nonsingular, the LTM can be singular only when the first three rows of the Jacobian have a rank less than 3. This implies that the top left 3×4 submatrix Js of ${}^2\mathbf{J}$ will have a rank less than 3 in a singular configuration. This sub-Jacobian is given by,

$$\mathbf{Js} = \begin{bmatrix} -a_4c_2s_3c_4 & a_4s_4 & -a_4s_3c_4 & -a_4c_3s_4 \\ a_4(s_2s_4+c_2c_3c_4)+a_2c_2 & 0 & a_4c_3c_4 & -a_4s_3s_4 \\ -a_4s_2s_3c_4 & -(a_2+a_4c_3c_4) & 0 & a_4c_4 \end{bmatrix}. \tag{26}$$

Denote by $\mathbf{J}_{ijk}$ the Jacobian formed by the i^{th}, j^{th}, and k^{th} columns of the Jacobian represented by Js. If the rank of Js is less than 3, then it follows that,

$$\det(\mathbf{J}_{123}) = 0, \quad \det(\mathbf{J}_{124}) = 0, \quad \det(\mathbf{J}_{134}) = 0, \quad \det(\mathbf{J}_{234}) = 0. \tag{27}$$

Based on the above conditions we obtain the singularities corresponding to a nonsingular wrist (see Table 3). Three singular configurations corresponding to a nonsingular wrist are shown in Fig. 2.

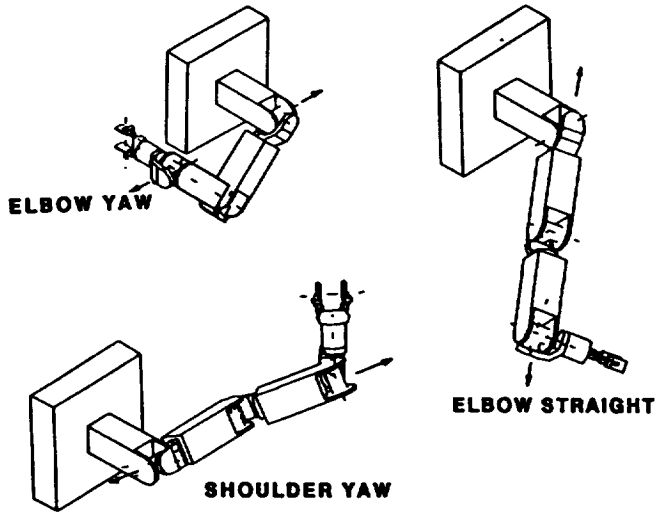

Table 3. Singularities of the LTM (Nonsingular Wrist)

θ_2	θ_3	θ_4	
	90	±90	
	-90	±90	NP2
w1		90	
w2		-90	
	0	0	
	180	0	NP1
	0	180	NP1
	180	180	
±90		0	
±90		180	

w1 = atan($-a_2/a_4$), w2 = atan(a_2/a_4)
NP1 -- Not possible. Link 2 is coincident with link 4.
NP2 -- Not possible. Wrist pitch, θ_3, is greater than –90.

Fig. 2 Singular configurations corresponding to a nonsingular wrist.

2. Joints 5 and 7 Are Collinear (Singular Wrist)

Notice that with joints 5 and 7 collinear ($\theta_6 = \pm 90°$), the two 6-dimensional vectors formed by columns 5 and 7 of Jacobian ${}^2\mathbf{J}$ are parallel, which corresponds to the wrist being in a singular position. Hence, for the LTM to have a singularity, only the sub-Jacobian given by the first six columns of ${}^2\mathbf{J}$ need be considered. This sub-Jacobian will be represented by Jss and can be written in the following form:

$$\mathbf{Jss} = \begin{bmatrix} -a_4c_2s_3c_4 & a_4s_4 & -a_4s_3c_4 & -a_4c_3s_4 & 0 & 0 \\ a_4(s_2s_4+c_2c_3c_4)+a_2c_2 & 0 & a_4c_3c_4 & -a_4s_3s_4 & 0 & 0 \\ -a_4s_2s_3c_4 & -(a_2+a_4c_3c_4) & 0 & a_4c_4 & 0 & 0 \\ -s_2 & 0 & 0 & s_3 & -c_3s_4 & c_3c_4s_5+s_3c_5 \\ 0 & 1 & 0 & -c_3 & -s_3s_4 & s_3c_4s_5-c_3c_5 \\ c_2 & 0 & 1 & 0 & c_4 & s_4s_5 \end{bmatrix}. \tag{28}$$

For the case under consideration, all the remaining singularities for the LTM can be determined by setting the determinant of the Jacobian Jss equal to zero. However, this leads to an equation for which the roots are difficult to determine. As a result, at this time only the singularities will be found that correspond to the occurrence of two sets of collinear joint axes. Since all singularities were found for which joints 5 and 7 were not collinear, then it follows that any singularities that occur due to two sets of collinear joint axes must have one of that set of collinear joint axes due to joints 5 and 7 being collinear. Thus to determine if two sets of collinear joint axes can occur, it is first necessary to find all possible cases where sets of joint axes are collinear. Then it must be determined if those sets can physically exist when joints 5 and 7 are collinear.

In the procedure for doing this we used the notation of Paul [6] in which the m^{th} joint axis lies along the z axis of the (m-1) frame. Thus, if the z axis of frame n is collinear with the z axis of frame m, it means that joint axes m + 1 and n + 1 are collinear. Let ${}^{m}T^{n}$ denote the homogeneous transform which refers frame n of the LTM to frame m of the LTM. To be collinear it follows that ${}^{m}T^{n}$ must be of the form

$$ {}^{m}T^{n} = \begin{bmatrix} r11 & r12 & 0 & 0 \\ r21 & r22 & 0 & 0 \\ 0 & 0 & \pm 1 & p3 \\ 0 & 0 & 0 & 1 \end{bmatrix}. \tag{29} $$

In general, the ${}^{m}T^{n}$ is of the form,

$$ {}^{m}T^{n} = \begin{bmatrix} r11 & r12 & r13 & p1 \\ r21 & r22 & r23 & p2 \\ r31 & r32 & \rho 33 & p3 \\ 0 & 0 & 0 & 1 \end{bmatrix}. \tag{30} $$

Thus, for two joint axes to be collinear, the following seven relations must be satisfied.

$$ \begin{array}{llll} \text{(a): } r13 = 0, & \text{(c): } r31 = 0, & \text{(e): } r33 = \pm 1, & \\ \text{(b): } r23 = 0, & \text{(d): } r32 = 0, & \text{(f): } p1 = 0, & \text{(g): } p2 = 0. \end{array} \tag{31} $$

Notice that Eq. (31) represents a set of dependent equations. Only Eqs. (31c), (31d), (31f), and (31g) are independent; however, the other equations help in the algebraic manipulation. Based on the above conditions, we obtain the singularities of the LTM when the wrist is in a singular configuration (Table 4). Figure 3 shows three of the singular configurations corresponding to a singular wrist. Including the singularities of both cases, that is, singular and nonsingular wrist, we obtain the singularities of the LTM shown in Table 5.

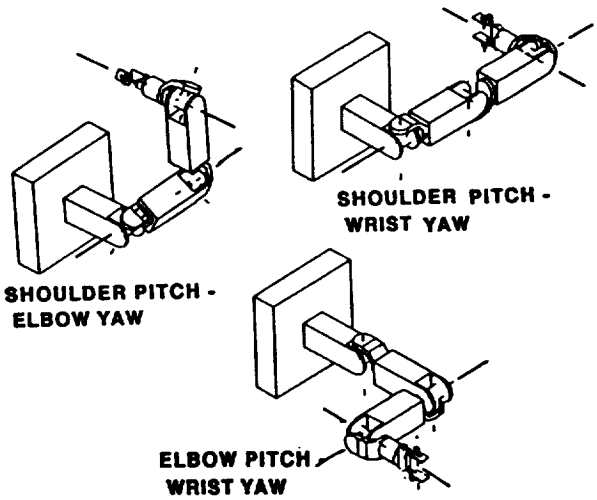

Fig. 3 Three configurations corresponding to a singular wrist.

Table 4. Singularities of the LTM (Singular Wrist)

θ_2	θ_3	θ_4	θ_5	θ_6
±90	90			0,180
		±90	90	0,180

Table 5. Singularities of the LTM (Singular and Nonsingular Wrist)

θ_2	θ_3	θ_4	θ_5	θ_6
	90	±90		
w1		90		
w2		-90		
	0	0		
	180	180		
±90		0		
±90		180		
±90	90			0,180
		±90	90	0,180

$w1 = \text{atan}(-a_2/a_4)$, $w2 = \text{atan}(a_2/a_4)$

To avoid the singular configurations shown in Table 5, we may optimize the following performance criterion:

$$H(\theta) = k_2\sin^2\theta_2 + k_3\cos^2\theta_3 + k_4\sin^2\theta_4 + k_6\cos^2\theta_6 , \quad (32)$$

where the k_i are weighting factors that may be chosen based on the range of the joint angle and the distance the joint angle is from its desired value. Inspection of Eq. (32) and Table 5 shows that if $H(\theta)$ is minimized, then joints 4 and 2 will tend to move toward 0° while joints 3 and 6 will tend to move toward ±90°.

6. Real-Time Implementation and Simulation Results

The robotic control scheme for the LTM is being implemented on a 16-MHz VME bus/Motorola 68020 microprocessor. The software is written in C language. Figure 4 is a block diagram of implementation of the kinematic optimization scheme. Control loops are closed around the joint servos, and the optimizing inverse kinematics algorithm is implemented in an open-loop fashion. The complete algorithm runs at 100 Hz, which includes the optimizing inverse kinematics, forward kinematics, joint-to-motor transformation calculations, and joint velocity and position limit checking.

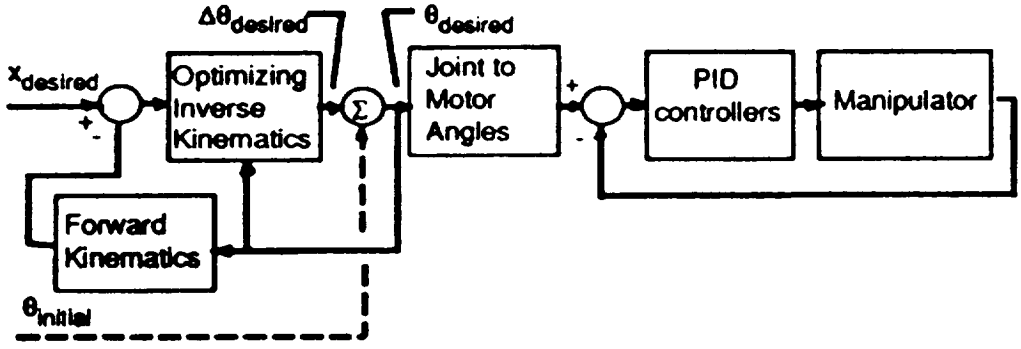

Fig. 4 Real-time implementation block diagram.

Graphical simulations to test the control software were performed for different cases. In each case the LTM end-effector follows a specified straight-line trajectory while maintaining a fixed orientation . In the first case, the performance criterion $H(\theta)$ in Eq. 24 is minimized so that the LTM avoids running into joint limits. In the second case, singularities are avoided by optimizing performance criterion $H(\theta)$ in Eq. 32. Comparison is made in each case with the joint trajectories resulting from the least-norm solution, which does not utilize the null space of the Jacobian to optimize a performance criterion.

Simulation results presented in Figures 5 and 6 are for the case when the performance criterion is optimized to avoid joint angle limits. Each figure shows the LTM trajectory along with a plot of joint angles as a function of time. In Fig. 5, only the least-norm solution is used to follow the desired end-effector trajectory. In this case joint 5 hits its lower limit before the end point is reached. Figure 6 demonstrates the use of redundancy to avoid the limits on joint angles. In this case the LTM reaches the desired end point along a specified trajectory without reaching a joint limit.

Figures 7 and 8 present the case when the performance criterion is optimized to avoid high joint velocities due to an internal singularity. The LTM is started in a near singular configuration in both figures. The least-norm solution shown in Fig. 7 produces high joint velocities and, therefore, the LTM is commanded to stop; however, Fig. 8 shows that if the null space of the Jacobian is utilized to avoid singularities, the desired end point is reached without getting too close to the singular configuration, thus avoiding high joint velocities.

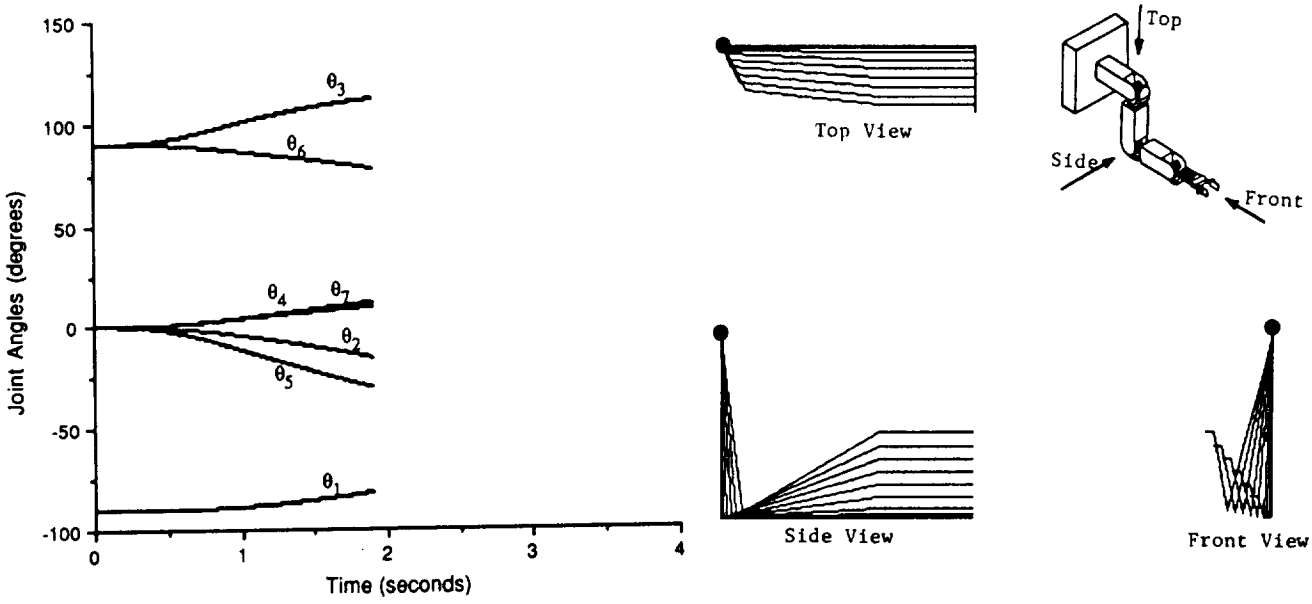

Fig. 5 End-effector motion along a straight line with a fixed orientation .
(Least-norm solution – reaches joint 5 limit)

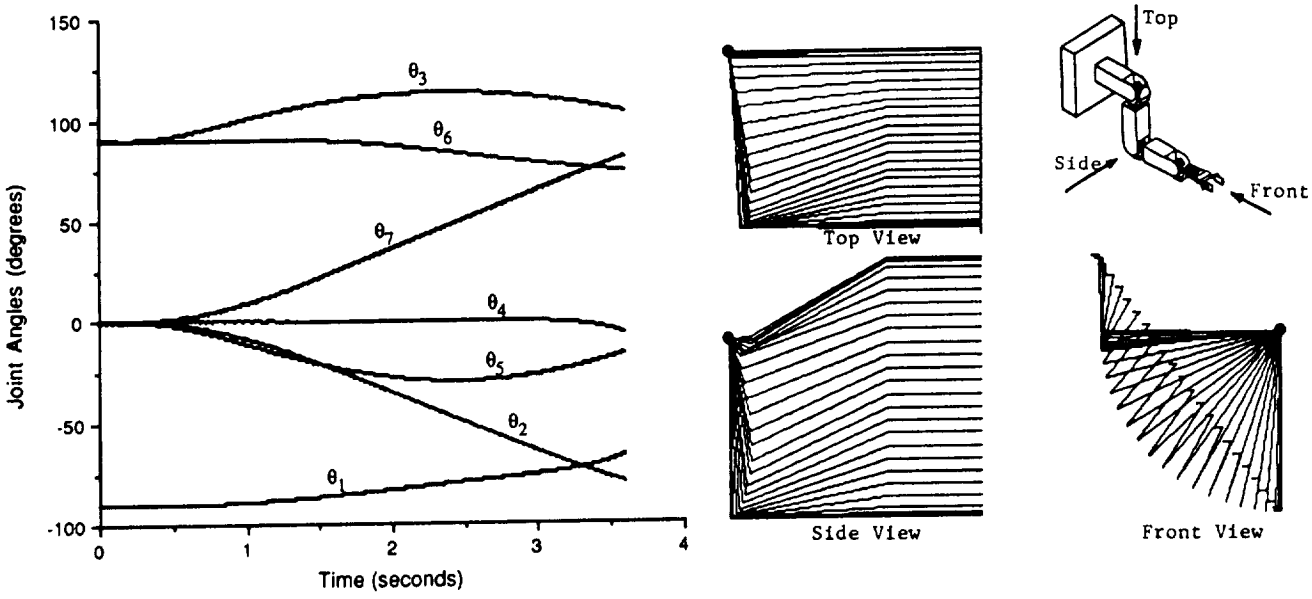

Fig. 6 End-effector motion along a straight line with fixed orientation.
(Redundancy utilized to avoid joint limits)

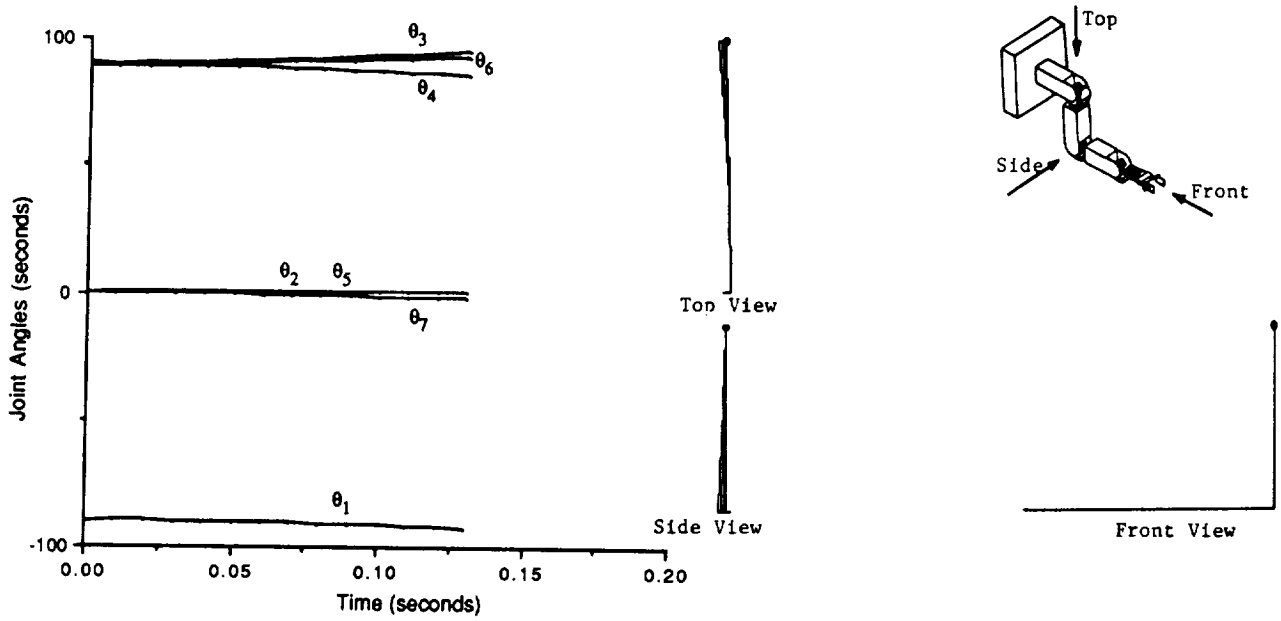

Fig. 7 End-effector motion along a straight line with a fixed orientation . (Least-norm solution–reaches velocity limit)

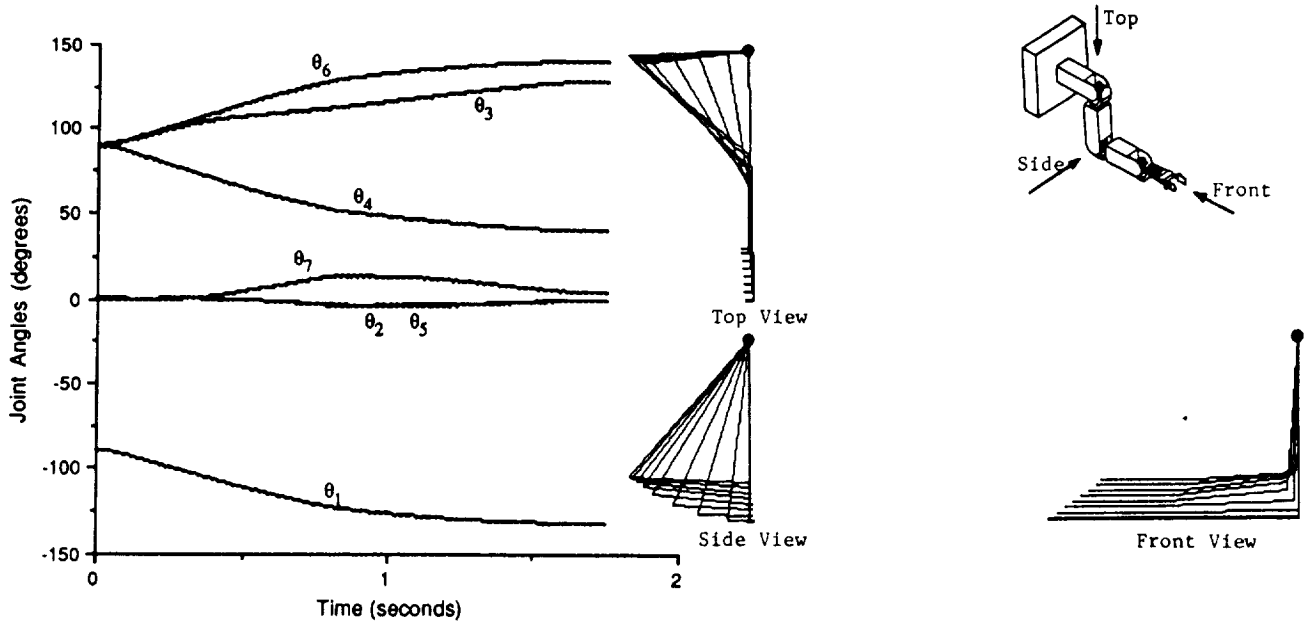

Fig. 8 End-effector motion along a straight line with a fixed orientation . (Redundancy utilized to avoid singularities)

7. Conclusions

A computationally efficient, robotic control scheme for the seven-degree-of-freedom LTM was presented. This scheme determines the joint velocities required to follow a specified end-effector trajectory while optimizing a given performance criterion using the gradient projection method. LTM kinematics was analyzed to determine its internal singularities. Performance criteria to avoid joint angle limits and singularities were obtained. Feasibility and effectiveness of the control scheme were demonstrated by simulations to avoid joint angle limits and singularities. Real-time implementation of the control scheme is in progress. Future work includes the use of redundancy to avoid obstacles and minimize joint torques, simultaneous optimizations of multiple performance criteria, and extension of the robotic control scheme to telerobotic control with force reflection.

References

[1] Herndon, J.N., Babcock, S.M., Butler, P.L., Costello, H.M., Glassell, R.L., Kress, R.L., Kuban, D.P., Rowe, J.C., Williams, D.M., "The Laboratory Telerobotic Manipulator Program," Proceedings of the NASA Conference on Space Telerobotics, January 31-February 2, 1989, Pasadena, California.

[2] Whitney, D. E., "The Mathematics of Coordinated Control of Prosthetic Arms and Manipulators," ASME J. Dynamic Systems, Measurement, and Control, 94, No. 4, 303-309 (1972)

[3] Dubey, R.V., Euler, J.A., and Babcock, S.M., "An Efficient Gradient Projection Optimization Scheme for a Seven-Degree-of-Freedom Redundant Robot with Spherical Wrist," Proc. of the IEEE International Conference on Robotics and Automation Philadelphia, April 1988, pp. 28-36.

[4] Albert, A., Regression and the Moore-Penrose Pseudo-Inverse, Academic Press, 1972.

[5] Liegeois, A., "Automatic Supervisory Control of the Configuration and Behavior of Multibody Mechanisms," IEEE Trans. Systems, Man, Cybern., SMC-7, No. 12 (1977)

[6] Paul, R.P., Robot Manipulators: Mathematics, Programming and Control, The MIT Press, 1981.

[7] Yoshikawa, T., "Manipulability of Robotic Mechanisms," The Int. J. of Rob. Research," Vol. 4, No. 2, Summer 1985, 3-9.